Comparison of UWB Radar Backscattering by the Human Torso and a Phantom

Melika Hozhabri, Per Olov Risman, Nikola Petrovic
Mälardalen University
Västerås, Sweden
Corresponding author's email address: melika.hozhabri@mdh.se

***Abstract*—An Ultra Wide Band (UWB) radar is used to measure the backscattering of a human and a human phantom. The choice of material and shape for the human phantom is discussed. The dielectric properties of the material (wet sand) used in the experiment are measured by a retromodeling technique and also calculated by mixture formulas. The appropriate frequency choice for the application is discussed.**

***Index Terms*—Ultra Wide Band, Radar, Human Detection, Phantom, Mie Scattering, Complex Permittivity**

I. Introduction

Remote detection of humans can have wide safety and security applications. The development of robotics and self driving vehicles impose a great risk to humans working in collaboration or in proximity to them. Technologies such as cameras, infra-red sensors as well as microwave systems are used for presence detection and localizing human beings. Microwave systems such as radars have advantages over other sensors as they enable seamless detection of humans during all weather and lighting conditions [1].

Among different radar sensors Ultra Wide Band (UWB) radar has shown some advantages such as good spatial resolution and high performance in multipath channels and delivers high signal to noise ratio (SNR) even in adverse conditions. UWB radar in free space is used to detect human by measuring small scale movements such as respiratory activity or heart rate [2], [3]. In [4], S. Chang, M. Wolf, and J. W. Burdick have used probability and statistical properties of a backscattered signal to detect and track human beings. All these methods need to log human activity for several seconds. This might not be acceptable for safety applications such as pedestrian collision avoidance. UWB radar transmitted signal has a large frequency spectrum which makes it difficult to gain frequency or phase information from the received signal. This may make UWB radar a less attractive candidate for discerning human beings from other objects.

The incident wave is diffracted, reflected and refracted by the target. A radar device is receiving the backscattered signal from the target. The signal characteristics depend on material (dielectric properties), size, shape, and incidence angle. A realistic phantom may assist to test and apply the same condition for human body electromagnetic field interaction across the frequency band of interest and makes it easier to replicate measurements. The dielectric properties of materials are obtained from their complex relative permittivity which is expressed as:

$$\varepsilon = \varepsilon' - j\varepsilon'' \tag{1}$$

where ε' is the relative permittivity and ε'' is the loss factor. The relation between the ionic contribution to the loss factor (ε''_σ) to the total conductivity is

$$\varepsilon''_\sigma = \frac{\sigma}{\omega\varepsilon_0} \tag{2}$$

where ε_0 is the absolute permittivity of free space and ω is the angular frequency.

The aim of this research is to investigate the possibility of using UWB radar for human detection for safety applications. In this research, a commercial UWB radar maximum length binary sequence (M-sequence) system from the Radarbolaget[1] company is used. This system is based on a time-of-arrival (TOA) ranging technique. The operational bandwidth is approximately 2 GHz (1–3 GHz). The platform consists of a radar processing unit (RPU) and a 14 bit analog to digital converter. The RPU is responsible for processing and synchronization of the signals. The system is equipped with two equal balanced micro-strip Vivaldi antennas. The transmit gain is adjustable and has a maximum value of –10 dBm. This particular radar system is described into detail in [5].

II. A human torso phantom

Humans have a complex surface profile and different body compositions and clothing which make them complicated targets. Measurements or numerical simulations are needed to gain understanding of electromagnetic scattering by complex objects. A simplified model of a person would separate the arms and legs from the trunk as different scattering objects. When measuring the Radar Cross Section (RCS) of a human being the main contribution is typically coming from the torso [6]. A circular cylinder with approximate height and circumference of an average human trunk, filled with materials with similar permittivity of human body, will thus be acceptable as a phantom.

The RCS of an object is related to the dielectric properties so it is important to have information about these. Various human body tissues have different relative permittivities which also

[1]Radarbolaget is located in Sweden and develops radar systems primarily for real time through wall monitoring of heating furnaces (http://www.radarbolaget.com/).

Fig. 1. Experimental setup

vary with frequency. C. Gabriel, S. Gabriel, and E. Corthout have presented human tissues dielectric properties in [7]. The stomach complex permittivity for 1.7 GHz (The geometric mean at 1−3 GHz) is ε = 63.4 + j0.27 obtained from [8].

For the phantom material a mixture of sand with fine grain sizes (0.1–0.7 mm) and water is chosen. Sand is selected because of its low ε' and since the water content after mixing is easy to measure. It is also inexpensive for the large volume needed. The chosen sand is light brown which is likely a combination of quartz with $\varepsilon' \approx 3.8$ and $\varepsilon'' \approx 0$ [9] and feldspar with with $\varepsilon' \approx 5.6$ and $\varepsilon'' \approx 0$ [10]. Water complex permittivity at 2.45 GHz is $\varepsilon_c = 78.72 + j10.76$ at 20°C obtained from [11], Table 6.1. Because the sand is mixed with water with much higher ε'', then the sand ε'' can be presumed to be zero and ε' is set to 5.

A. Using A Mixture Formula to Calculate the Wet Sand Permittivity

The density of dry sand is measured by the water displacement method which yields 2500 $\mathrm{kg/m^3}$. The wet sand mixture is filled approximately up to 915 mm of the pipe with 95.6 kg of sand, which means that the sand packing density is around 53 %.

To predict the permittivity of water and sand the mixture formula from a review by Kraszewski [12] is used. The simplified Looyenga equation may satisfy our application,

$$\varepsilon_m = [\varepsilon_c^{1/2} + v_i(\varepsilon_i^{1/2} - \varepsilon_c^{1/2})]^2 \tag{3}$$

where ε_c and ε_i are complex permittivities of the two components and v_c and v_i are their volumetric properties with $v_c + v_i = 1$. ε_c is the permittivity of the medium surrounding the particulates. The result of the calculations is shown in Table I.

B. Measurement of the Complex Permittivity of Wet Sand

The degenerate resonance method, which is a retromodeling technique, is used to calculate the complex permittivity of wet sand (chapter 5.6 in [11]). The measurement cavity consists of a large aluminum tube with a welded "chimney" for sample container insertion (see Fig.2). The system is modeled

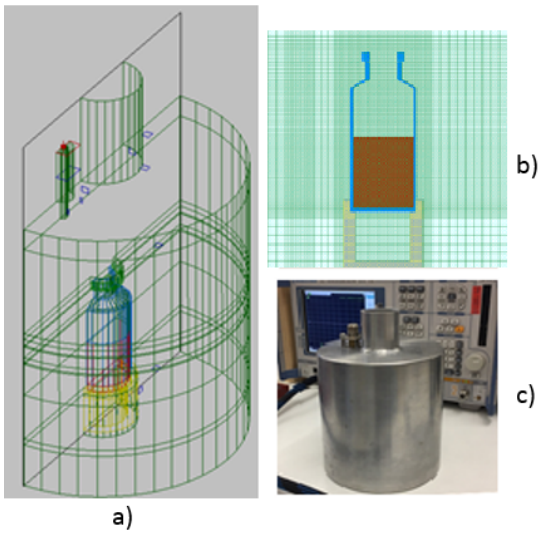

Fig. 2. (a) The measurement cavity, from the software editor. Since the system is symmetrical along a vertical plane only half of it needs to be modeled. (b) The glass container (blue) with the material under test (MUT) (red) stands on a PTFE support which enhances the sensitivity. (c) The cavity.

geometrically by the numerical FDTD software QWED [13]. A vector network analyzer (VNA) from Rohde & Schwarz model ZVB-8 is used to measure the reflection coefficient amplitude as a function of frequency. The measurements are done firstly with just the sample container and then with the sample in the container. The frequency range in this case is (2450±100) MHz. A start (guess) complex permittivity value of the sample is then introduced, and then changed to obtain an agreement with the measured values.

This method yields $\varepsilon' = 18$ and $\sigma = 2$. ε'' can be calculated by (2) which yields ε'' = 14.7 at 2.45 GHz. The measured ε'' is much larger than the value calculated from the mixture formula. A reason can be the Maxwell–Wagner effect, caused by charge redistributions on the sand particles, since sand has a very low conductivity and the sand particles are contacting each other.

III. Torso Measurement

A PVC (Polyvinyl Chloride) sewage pipe 315 mm × 1200 mm and thickness 9.2 mm is used to simulate a human torso (see Fig. 1). The pipe is filled with the sand–water mixture.

The transmitting and receiving antennas are placed 800 mm from the ground with 500 mm in between on an expanded polystyrene stand; this creates a 28° angle, so actual backscattering is not measured. The objects are placed 2.00 m away

TABLE I
COMPLEX PERMITTIVITY OF WET SAND

Method	ε'	ε''
Measurement	18	14.7
Looyenga mixture formula	28.7	3.7

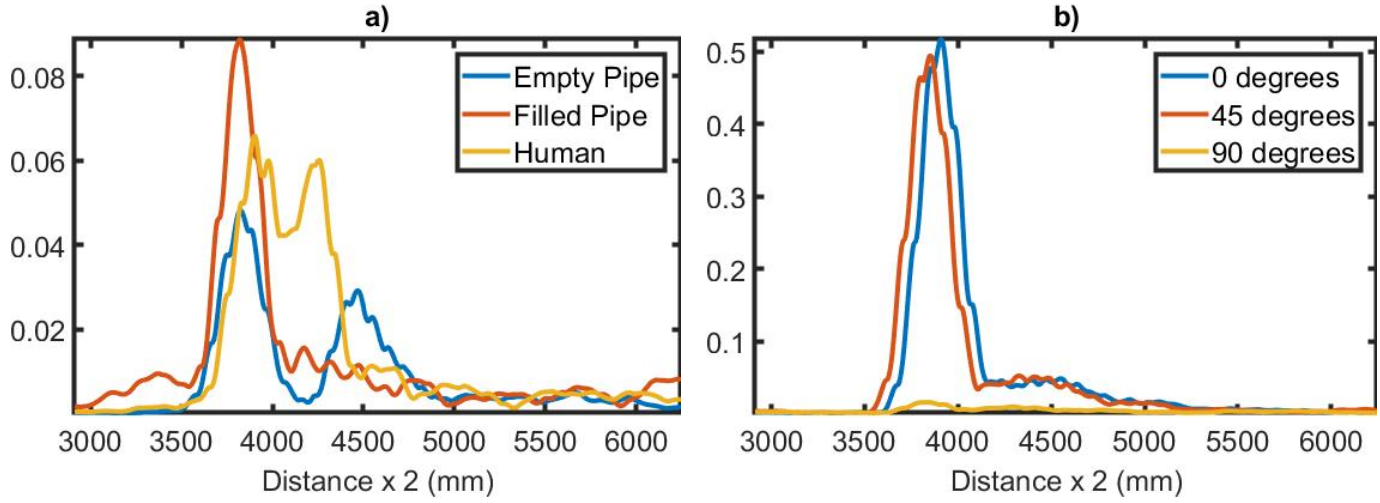

Fig. 3. (a) Processed RCS of empty pipe, sand filled pipe and human in vicinity of UWB radar. (b) A metal plate measurement with different polarization of receiver antenna.

from the antenna pair. A 360 degree circular plastic protractor ruler with adjustable angle is used to change the polarization of the transmitter antenna (not the receiver antenna). The polarization is set to 0°, 45°, and 90° where 0° is when E field is parallel with the object axis.

IV. Results and Discussion

Fig.3 shows the received radar signal. The horizontal axis represents the time of flight, which is recalculated to twice the distance to the test object. The distance between two adjacent measurement points in horizontal axis is $22\,367.7\,\mathrm{ns}$ corresponds to $4166.7\,\mu\mathrm{m}$. The vertical axis shows the received signal, correlated by the transmitted signal in the RPU. All measured raw signals signal are rectified and a moving average algorithm is then applied using a sliding window equivalent to 201 mm in length.

The RCS of an adult man with his back towards the antenna is shown in yellow in Fig. 3. a. The RCS has two distinct maxima, around 150 mm apart in distance. This can be a discerning of the horizontal distance between back of the head and the shoulders. The empty pipe vertical RCS shown in blue has two maxima at about 300 mm distance (more exactly 330±10 mm) and can be due to scattering from the pipe front and back.

The filled pipe vertical RCS shown in red is larger than the human RCS. This can simply be due to the smaller heights at different distances in the human case, i.e the overall summed signals from the pipe and torso are about the same. That is also seen in the Fig. 3. a.

The metal plate RCS is shown in different antenna polarizations of the transmitter antenna, with 0° is when E field is parallel with the object axis in Fig. 3. b. In case of 0° and 45° polarizations the RCS has almost the same amplitude. The graphs are slightly shifted which might be due to the small errors in manual adjustment of the antennas during the measurements.

Fig. 4 shows the theoretical RCS of a homogeneous perfectly conducting metal sphere. The horizontal axis scaling is the quotient of sphere radius to the radar wavelength: r/λ. The RCS of a cylinder has very similar properties. When the circumference of the object is comparable with the incident wavelength, interesting effects such as surface wave phenomena occur, and will blur the RCS [11].

One has to observe the possibility of blurring of the time of flight measurements by any diffraction phenomena in the Mie region in Fig. 4, but this shows that there should not be any such problems in the present case. Another possibility of blurring is excitation of internal resonances, in particular in the wet sand pipe case. Using the usual formula for penetration depth for the wet sand at (say) 1.7 GHz, one obtains about 40 mm in the worst case in Table I. Since this is much less than the pipe radius, no such phenomena occurs in the present case.

As mentioned before, this UWB radar system operating frequency is between 1 and 3 GHz, so the wavelength is approximately between 0.1 and 0.3 meters. If an average human torso is estimated as a cylinder with 90 cm circumference, then the value of r/λ equals from 1.5 to 3.15, which is in the optical region. In Mie resonance region, the cross section is approximately 3 times larger, which means that an object of the size and geometry of human body torso will have the best discerning in that region.

V. Conclusions

It is shown that the UWB system at 1–3 GHz used in this work provides possibilities to detect the breast/neck/head distance differences under the quite idealized undisturbed conditions, at a target distance of some few meters. With an electromagnetically similar object – wet sand in a 300 mm diameter plastic pipe – a discernibly different signal was obtained. It is, however, questioned if a leaning human can be sufficiently discerned or if detection from a higher elevation

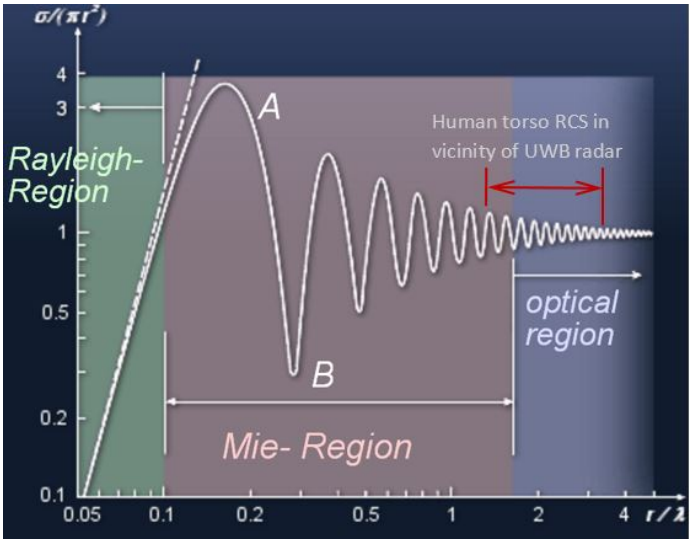

Fig. 4. Monostatic radar cross section (RCS) of a perfectly conducting metal sphere as a function of frequency, calculated by Mie theory [14].

is feasible.

VI. Future Work

Additional possibilities such as use of lower frequencies in the Mie region seem interesting, as does much higher frequencies, then for quasi-optical movement pattern recognition by added statistical or similar algorithms. The relationships between object radius (or rather and more generally: the circumference) at maximum "A" and minimum "B" in Fig. 4 are interesting to study, by simultaneous use towards discerning of human torso or legs. The lowest microwave frequencies must then be employed, so the spatial resolution of exact human locations will then be an issue.

References

[1] J. A. Nanzer, "A review of microwave wireless techniques for human presence detection and classification," *IEEE Transactions on Microwave Theory and Techniques*, vol. 65, pp. 1780–1794, May 2017.

[2] G. Shingu, K. Takizawa, and T. Ikegami, "Human body detection using mimo-uwb radar sensor network in an indoor environment," in *2008 Ninth International Conference on Parallel and Distributed Computing, Applications and Technologies*, pp. 437–442, Dec 2008.

[3] Y. Kilic, H. Wymeersch, A. Meijerink, M. J. Bentum, and W. G. Scanlon, "An experimental study of uwb device-free person detection and ranging," in *2013 IEEE International Conference on Ultra-Wideband (ICUWB)*, pp. 43–48, Sept 2013.

[4] S. Chang, M. Wolf, and J. W. Burdick, "Human detection and tracking via ultra-wideband (uwb) radar," in *2010 IEEE International Conference on Robotics and Automation*, pp. 452–457, May 2010.

[5] M. Hozhabri, M. Otterskog, N. Petrovic, and M. Ekström, "Experimental comparison study of uwb technologies for static human detection," in *2016 IEEE International Conference on Ubiquitous Wireless Broadband (ICUWB)*, pp. 1–4, Oct 2016.

[6] T. Dogaru, L. Nguyen, and C. Le, *Computer models of the human body signature for sensing through the wall radar applications*. Army Research Laboratory Adelphi, MD, 2007.

[7] C. Gabriel, S. Gabriel, and E. Corthout, "The dielectric properties of biological tissues: I. literature survey," *Physics in Medicine & Biology*, vol. 41, no. 11, p. 2231, 1996.

[8] R. D.Andreuccetti and C.Petrucci, "An internet resource for the calculation of the dielectric properties of body tissues in the frequency range 10 hz - 100 ghz,ifac-cnr, florence (italy), 1997. based on data published by c.gabriel et al. in 1996. [online]. available:http://niremf.ifac.cnr.it/tissprop/."

[9] P. Sarafis and A. G. Nassiopoulou, "Dielectric properties of porous silicon for use as a substrate for the on-chip integration of millimeter-wave devices in the frequency range 140 to 210 ghz," *Nanoscale Research Letters 9.1*, p. 418, 2014.

[10] Y. Zheng, S. Wang, J. Feng, Z. Ouyang, and X. Li, "Measurement of the complex permittivity of dry rocks and minerals: application of polythene dilution method and lichtenecker mixture formula," *Geophysical Journal International*, vol. 163, pp. 1195–1202, Dec 2005.

[11] M. Lorence and P. Pesheck, *Development of Packaging and Products for Use in Microwave Ovens*. Woodhead Publishing in Materials, Elsevier Science, 2009.

[12] A. Kraszewski, "Prediction of the dielectric properties of two-phase mixtures," *Journal of Microwave Power*, vol. 12, no. 3, pp. 216–222, 1977.

[13] . Quickwave™, www.qwed.eu.

[14] "http://www.radartutorial.eu/01.basics/rayleigh-[accessed 25,6,2018]."